

## ELASTIC PHOTON SCATTERING AND PHOTOEFFECT BY K-SHELL ELECTRONS IN NEUTRAL ATOMS\*

A. COSTESCU<sup>1</sup>, M. MOLDOVAN<sup>1,2</sup>, S. SPANULESCU<sup>3</sup>, C. STOICA<sup>1</sup>

<sup>1</sup>Department of Physics, University of Bucharest, P.O.Box MG-11, Bucharest-Magurele 077125, Romania, Email: a\_costescu@hotmail.com; Email: cr\_stoica@yahoo.com

<sup>2</sup>Department of Physics, UMF Targu Mures, Gh. Marinescu 38, Targu Mures 540142, Romania, E-mail: mirceamld@yahoo.co.uk

<sup>3</sup>Department of Physics, “Hyperion” University of Bucharest, Calarasilor 169, Bucharest 030629, Romania, E-mail: severspa2004@yahoo.com

Received September 20, 2010

*Abstract.* A screening model based on nonrelativistic Hartree-Fock central field is elaborated for the K-shell Rayleigh amplitudes and the total photoeffect cross section. It is valide in a large energy range from a few hundred eV up to hundreds of keV for intermediate and large atomic numbers. Multipoles, retardation as well as relativistic kinematics effects are taken into account. A good agreement with full relativistic numerical calculations is found.

*Key words:* elastic scattering, photoeffect, effective charge, Hartree-Fock charge distribution.

### 1. INTRODUCTION

The use of x and soft  $\gamma$  ray beams has been of fundamental importance in investigating the structure of matter (gases, liquids, solids) as well as most of its physical properties. Also, the elastic photon scattering is among the processes (photoeffect, pair production, inelastic Compton scattering) responsible for attenuating photon beams in matter. Significant advances in the use of synchrotron sources that allow obtaining large intensities of high energy photons beams made possible to perform more and more accurate experiments. Major advances in the development of computer codes that calculate the relativistic S-matrix for Rayleigh [1, 2] and Compton scattering [3] permitted to perform precise numerical calculations for the cross sections that describe atomic x-ray and  $\gamma$ -ray scattering. Significant theoretical results were also obtained in the photon energy range above a few hundred eV up to  $\alpha Zm$  for Rayleigh [4] and Compton [5, 6] scattering. These theoretical calculation well beyond the usual form factor (for Rayleigh) and

---

\* Paper presented at the Annual Scientific Session of Faculty of Physics, University of Bucharest, June 18, 2010, Bucharest-Magurele, Romania.

impulse approximations (for Compton) show that in the considered energy range all contributions from multipoles, retardation and relativistic kinematics are needed, but they were performed for the K-shell electrons in the case of a Coulomb field. The aim of this paper is to extend our theoretical results to the full realistic case of the photon scattering by inner shell electrons of neutral atoms.

We want to take advantage of our coulombian formulae which describe with high accuracy the dynamic effects due to retardation and relativistic effects [4]. For that we consider that important atomic features due to the internal structure are well described as independent atomic electrons interacting electrostatically with a single screened central potential given by the coulombian field of the nucleus and the charge distribution of all the atomic electrons. This represents the main approximation in the description of the atom, which is assumed to be spherically symmetric and with the electron-electron interactions included only within the independent particle approximation (IPA) and local exchange approximations. The IPA is sure correct if the photon energies are sufficiently high so that effects due to electron-electron correlation are small enough to be neglected for the photon scattering process. To the elastic scattering of photons by the atom contributes each individual bound electron which elastically scatters the incident photon. Because the energy of the scattered photon is the same as that of the incoming photon it is not possible to know which of the bound electrons is responsible for the scattering. As a consequence we have to perform the coherent sum of the amplitudes and then to square to obtain the elastic scattering cross section of the whole atom.

## **2. RAYLEIGH SCATTERING AND PHOTOEFFECT FOR HYDROGEN-LIKE ATOMS IN THE CASE OF THE K-SHELL ELECTRONS**

The nonrelativistic limit of the second order S-matrix element for elastic scattering of photons by K-shell electrons has been calculated some time ago for hydrogen-like atoms [4]. The procedure could be applied to neutral atoms if their effective atomic number  $Z_{\text{ef}}$  is known, considering the screening effects of the others electrons. For the K shell these screening effects on the charge distribution are not so large but for other shells it may be very important.

We use the effective charge approximation which replaces the wave function of the non ionized atoms with the hydrogen-like wave functions corresponding to an “effective” atomic number  $Z_{\text{ef}}$ . It is obtained by fitting the Hartree-Fock wave function of the many body case with a hydrogen-like one given by an appropriate effective charge  $Z_{\text{ef}}$ , as we will present further. Within this approach the formulae obtained earlier [4] for the K-shell remain valid and in this way we keep all the expressions which describe with high accuracy multipoles, retardation and relativistic kinematics effects.

In the second order of the perturbation theory, the S matrix element involves the sum over all intermediate states. In the case of two photon processes there are two Feynman diagrams, each of them containing a coulombian Green function  $G(\Omega)$  where  $\Omega$  is the energy of the virtual electron. In the case of elastic scattering of photons by K-shell electrons,

$$\Omega_1 = E_0 + \omega; \quad \Omega_2 = E_0 - \omega, \quad (2.1)$$

where  $E_0 = \gamma m$ , with  $\gamma = (1 - \alpha^2 Z^2)^{\frac{1}{2}}$ , is the ground state energy and  $\omega$  is the photon energy.

The coulombian Green function involves the parameter

$$\tau = \frac{\alpha Z \Omega}{\sqrt{m^2 - \Omega^2}}, \quad (2.2)$$

which describes the coulombian interaction.

It was proved [5] that the right way for obtaining the nonrelativistic limit of two photon matrix element is to include all multipoles, retardation and relativistic kinematics terms and only after all the algebraic calculations are performed the limit may be correctly obtained.

By systematically neglecting the higher order terms in  $\frac{\omega}{m}$  we obtain the nonrelativistic expressions for the parameter  $\tau$  as

$$\tau_1^{\text{nr}} = \begin{cases} (1 - \omega/\omega_{1s})^{-\frac{1}{2}}, & \omega < \omega_{1s} \\ i(\omega/\omega_{1s} - 1)^{-\frac{1}{2}}, & \omega_{1s} \leq \omega \ll \omega_{pp} \end{cases} \quad (2.3)$$

$$\tau_2^{\text{nr}} = (1 + \omega/\omega_{1s})^{-\frac{1}{2}}, \quad \omega \ll \omega_{pp} \quad (2.4)$$

where

$$\omega_{1s} = (1 - \gamma)m; \quad \omega_{pp} = (1 + \gamma)m. \quad (2.5)$$

The Rayleigh amplitudes may be written in terms of the invariant amplitudes

$$M^{\text{R}} = M(\omega, \theta) (\vec{s}_1 \vec{s}_2) + N(\omega, \theta) (\vec{s}_1 \vec{v}_2) (\vec{s}_2 \vec{v}_1), \quad (2.6)$$

where

$$M(\omega, \theta) = \mathcal{O} - P(\Omega_1, \theta) - P(\Omega_2, \theta), \quad (2.7)$$

$$N(\omega, \theta) = -Q(\Omega_1, \theta) - Q(\Omega_2, \theta), \quad (2.8)$$

where  $\mathcal{O}$  the atomic form factor which has the nonrelativistic limit

$$\mathcal{O} = \left(1 + \frac{\alpha^2 Z^2}{4} \frac{\omega^2}{\omega_{1s}^2} \sin^2 \frac{\theta}{2}\right)^{-2}. \quad (2.9)$$

We want to mention that the invariant amplitudes  $P(\Omega, \theta)$  and  $Q(\Omega, \theta)$  are given by the sum over all positive frequencies contained in the coulombian Green function. Due to the different expressions of some parameters for energies below and above

the photoeffect threshold, the amplitudes  $P(\Omega, \theta)$  and  $Q(\Omega, \theta)$  are differently written for the two cases. For photon energies below  $\omega_{1s}$ , these amplitudes are

$$P_{nr}(\Omega, \theta) = 2^3 (\alpha Z)^8 \frac{m^4}{\omega_{1s}^4} \left(1 \mp \frac{\omega}{\omega_{1s}}\right)^{\frac{3}{2}} \frac{1}{D^2} \frac{F_1(2-\tau^{nr}; 2, 2; 3-\tau^{nr}; x_1^{nr}, x_2^{nr})}{2-\tau^{nr}}, \quad (2.10)$$

$$Q_{nr}(\Omega, \theta) = 2^5 (\alpha Z)^{10} \frac{m^4}{\omega_{1s}^4} \frac{\omega^2}{\omega_{1s}^2} \left(1 \mp \frac{\omega}{\omega_{1s}}\right)^{\frac{5}{2}} \frac{1}{D^3} \frac{F_1(3-\tau^{nr}; 3, 3; 4-\tau^{nr}; x_1^{nr}, x_2^{nr})}{3-\tau^{nr}}, \quad (2.11)$$

where the denominators  $D$  are given by the relationship

$$D = \left[ \left(1 + \frac{E_0}{m}\right) \left(1 + \sqrt{1 \mp \frac{\omega}{\omega_{1s}}}\right) \mp \frac{E_0}{m} \frac{\omega}{\omega_{1s}} \right]^2 \pm \alpha^2 Z^2 \frac{\omega}{\omega_{1s}}. \quad (2.12)$$

The Appell's functions  $F_1$  may be calculated from their integral representation

$$\frac{F_1(b-\tau; b, b, b+1-\tau; x_1, x_2)}{b-\tau} = \int_0^1 d\rho \frac{\rho^{b-\tau-1}}{(1-s\rho+p\rho^2)^b}, \quad (2.13)$$

with  $b = 2, 3$ . Their variables satisfy the relationships

$$p \equiv x_1 x_2 = \xi^2(\Omega) \quad (2.14)$$

$$s \equiv x_1 + x_2 = 2 \left[ 1 - 2\alpha^2 Z^2 \left(1 - \frac{\omega}{\omega_{1s}}\right) \sin^2 \frac{\theta}{2} \right] \xi(\Omega) \quad (2.15)$$

and  $\xi(\Omega)$  is given by

$$\xi(\Omega) = \frac{1}{D} \left( \frac{\omega}{\omega_{1s}} \right)^2. \quad (2.16)$$

For photon energies above the K shell threshold energy the parameter  $\xi(\Omega)$  is given by

$$\xi(\Omega) = \frac{1 + \frac{\omega}{\alpha^2 Z^2 m} - \left(1 + \frac{\omega}{\omega_{1s}}\right)^{\frac{1}{2}}}{1 + \frac{\omega}{\alpha^2 Z^2 m} + \left(1 + \frac{\omega}{\omega_{1s}}\right)^{\frac{1}{2}}} \quad (2.17)$$

and the nonrelativistic limit of the amplitudes may be written

$$P_{nr}(\Omega, \theta) = 2^3 (\alpha Z)^8 \frac{m^4}{\omega^4} \xi^2(\Omega) \left( \frac{\omega}{\omega_{1s}} \mp 1 \right)^{\frac{3}{2}} \frac{F_1(2-\tau^{nr}; 2, 2; 3-\tau^{nr}; x_1^{nr}, x_2^{nr})}{2-\tau^{nr}}, \quad (2.18)$$

$$Q_{nr}(\Omega, \theta) = \mp 2^5 (\alpha Z)^{10} \frac{m^4}{\omega^4} \xi^3(\Omega) \left( \frac{\omega}{\omega_{1s}} \mp 1 \right)^{\frac{5}{2}} \frac{F_1(3-\tau^{nr}; 3, 3; 4-\tau^{nr}; x_1^{nr}, x_2^{nr})}{3-\tau^{nr}}. \quad (2.19)$$

It is possible to obtain the imaginary part of the invariant amplitudes  $P_{nr}(\Omega)$  and  $Q_{nr}(\Omega)$  in terms of elementary functions as follows

$$\begin{aligned} \text{Im} P_{nr}(\Omega_1, \theta) &= 2\pi (\alpha Z)^4 \frac{E_0}{\omega} \frac{\Omega_1}{\omega} \frac{\omega_{1s}}{\omega} \frac{m}{\omega} \frac{e^{-|\tau_1^{nr}|[\pi + \chi_{nr}(\omega)]}}{1 - e^{-2\pi|\tau_1^{nr}|}} \frac{1}{1 + \alpha^2 Z^2 \left(\frac{\omega}{\omega_{1s}} - 1\right) \sin^2 \left(\frac{\theta}{2}\right)} \\ &\times \frac{1}{\sin^2 \left(\frac{\theta}{2}\right)} \left[ \frac{1 + 2\alpha^2 Z^2 \left(\frac{\omega}{\omega_{1s}} - 1\right) \sin^2 \left(\frac{\theta}{2}\right)}{2\alpha Z \sqrt{1 + \alpha^2 Z^2 \left(\frac{\omega}{\omega_{1s}} - 1\right) \sin^2 \left(\frac{\theta}{2}\right)}} \frac{\sin(w)}{\sin \left(\frac{\theta}{2}\right)} - \cos(w) \right] \end{aligned} \quad (2.20)$$

$$ImQ_{nr}(\Omega_1, \theta) = \frac{3\pi}{2}(\alpha Z)^4 \frac{E_0}{\omega} \frac{\Omega_1}{\omega} \frac{\omega_{1s}}{\omega} \frac{m}{\omega} \frac{1+2|v_{nr}|}{(1+|v_{nr}|)^2} \frac{1}{\sin^4(\frac{\theta}{2})} \frac{e^{-|\tau_1^{nr}|[\pi+\chi_{nr}(\omega)]}}{1-e^{-2\pi|\tau_1^{nr}|}}$$

$$\times \left\{ \frac{1}{2\alpha Z} \frac{1}{\sqrt{1+|v_{nr}|}} \left[ 1 + \frac{2}{3}|v_{nr}| + \frac{4}{3} \frac{|v_{nr}|^2}{1+2|v_{nr}|} - \frac{4}{3} \alpha^2 Z^2 \frac{1+|v_{nr}|}{1+2|v_{nr}|} \sin^2 \frac{\theta}{2} \right] \frac{\sin(w)}{\sin(\frac{\theta}{2})} - \cos(w) \right\} \quad (2.21)$$

with

$$w = 2 \left( \frac{\omega}{\omega_{1s}} - 1 \right)^{-\frac{1}{2}} \ln \left( \sqrt{1+|v_{nr}|} + \sqrt{|v_{nr}|} \right) ; |v_{nr}| = \alpha^2 Z^2 \left( \frac{\omega}{\omega_{1s}} - 1 \right) \sin^2 \left( \frac{\theta}{2} \right), \quad (2.22)$$

For the forward scattering ( $\theta = 0$ ) the equation (2.20) becomes

$$ImP_{nr}(\Omega_1, \theta = 0) = 2\pi(\alpha Z)^4 \frac{E_0}{\omega} \frac{\Omega_1}{\omega} \frac{\omega_{1s}}{\omega} \frac{m}{\omega} \frac{e^{-|\tau_1^{nr}|[\pi+\chi_{nr}(\omega)]}}{1-e^{-2\pi|\tau_1^{nr}|}}, \quad (2.23)$$

where

$$\chi_{nr}(\omega) = \begin{cases} -\pi + 2 \arctan \left( \frac{\sqrt{\frac{\omega}{\omega_{1s}} - 1}}{1 - \frac{E_0 \omega}{\alpha^2 Z^2 m^2}} \right), & \text{if } \omega \leq \frac{\alpha^2 Z^2 m^2}{E_0} \\ \pi - 2 \arctan \left( \frac{\sqrt{\frac{\omega}{\omega_{1s}} - 1}}{-1 + \frac{E_0 \omega}{\alpha^2 Z^2 m^2}} \right), & \text{if } \omega > \frac{\alpha^2 Z^2 m^2}{E_0}. \end{cases} \quad (2.24)$$

We introduce the amplitudes perpendicular ( $A^\perp$ ) and parallel ( $A^\parallel$ ) to the scattering plane,

$$A^\perp(\omega, \theta) = M(\omega, \theta) \text{ and } A^\parallel(\omega, \theta) = M(\omega, \theta) \cos \theta - N(\omega, \theta) \sin^2 \theta. \quad (2.25)$$

According to the optical theorem, the total cross section for the photoeffect is associated to the imaginary part of the forward Rayleigh scattering amplitude ( $\theta = 0$ ) with the specification  $\vec{s}_1 = \vec{s}_2$ :

$$\sigma^{ph} = \frac{4\pi}{\alpha} \frac{m}{\omega} r_0^2 |ImM(\omega, \theta = 0)| = \frac{4\pi}{\alpha} \frac{m}{\omega} r_0^2 |ImP_{nr}(\Omega_1, \theta = 0)| \quad (2.26)$$

Using the relationship (2.23) we get

$$ImP_{nr}(\Omega_1, \theta) = \frac{8\pi}{3}(\alpha Z)^6 \frac{\Omega_1}{\omega} \frac{E_0}{\omega} \frac{m}{\omega} \frac{e^{-|\tau_1^{nr}|[\pi+\chi_{nr}(\omega)]}}{e^{\pi|\tau_1^{nr}|} - e^{-\pi|\tau_1^{nr}|}} {}_2F_1 \left( 2 - \tau_1^{nr}; 2 + \tau_1^{nr}; \frac{5}{2}; v_{nr} \right) \quad (2.27)$$

and we obtain the total photoeffect cross section in the nonrelativistic limit:

$$\sigma_{1s}^{ph} = \frac{32}{3} \pi^2 r_0^2 E_0 m^2 \alpha^5 Z^6 \frac{E_0 + \omega}{\omega^4} \frac{e^{-|\tau_1^{nr}|[\pi+\chi_{nr}(\omega)]}}{1-e^{-2\pi|\tau_1^{nr}|}}. \quad (2.28)$$

The predictions provided by this formula [4] are in good agreement with the full relativistic numerical calculations [7, 8] for intermediate and high values of the atomic number and incident photon energies at least twice the threshold energy. This shows that spin effects are indeed small in the case of photon energies up to  $\alpha Z m$ .

### 3. THE DYNAMIC SCREENING MODEL FOR K-SHELL RAYLEIGH SCATTERING AND PHOTOEFFECT CROSS SECTIONS

#### 3.1. RAYLEIGH SCATTERING

In order to take into account the effects of screening on processes involving the interaction of atomic electrons with photons, it is needed to know the charge distribution for each electron of the atom. The usual procedure consists of considering each electron as being under the influence of a central field due to the nucleus and all other electrons of the atom. The Hartree-Fock model is using this assumption, and consequently, all electrons of the same atomic subshell are under the influence of the same central field, with the same energy and the same charge distribution. In particular, the Hartree-Fock model, like any model based on IPA, should lead to a very good description of screening for inner electrons, *i.e.* the electrons of the atomic subshells 1s, 2s and 2p.

The screening problem is more complicated when a scattering process of photons by atomic electrons is considered, because distances where the particles interact depend on the momentum transfer  $|\vec{\Delta}|$  between the interacting particles. That is why, the electric charge “seen” by the electron in the interacting point depends on the energy  $\omega$  and the scattering angle  $\theta$  of the photon. Thus, any screening model that is associated to a specific process of interaction has a specific dynamics, unlike the usual Hartree-Fock problem where the static charge distribution and the orbital energy of each atomic subshell has to be achieved. As we can note from the Fig. 1, the Hartree-Fock model shows an almost linear dependence on the distance from the nucleus of the negative charge distribution.

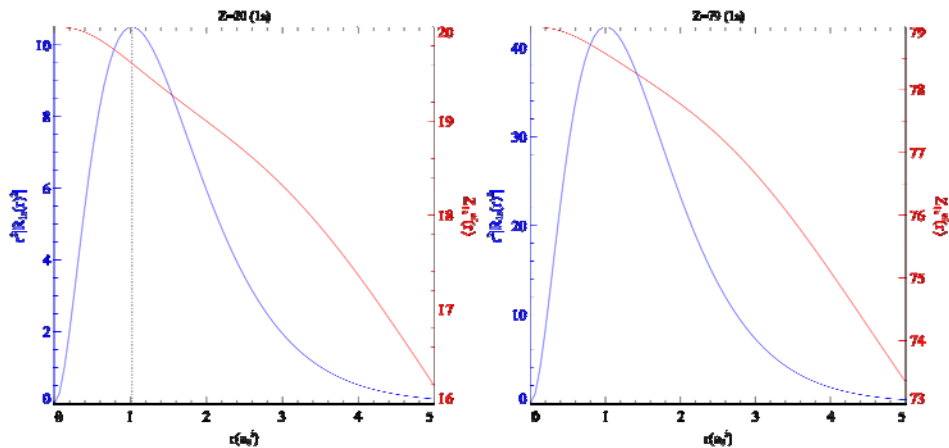


Fig. 1 – The effective charge and the Hartree-Fock charge density for the 1s electron, in the case of Calcium ( $Z=20$ ) and Gold ( $Z=79$ ). The distance  $r$  is expressed in ion Bohr radius  $a_0^{-1} = (\alpha Z m)^{-1}$ .

Based on the very good predictions which can be obtained in the nonrelativistic limit, even in the case of energy of tens and hundreds keV in the case of Compton effect, Rayleigh effect or photoeffect on 1s of hydrogen-like ions, we would like to extend the analytical expressions to the neutral atoms case. In order to achieve that, it is obvious that the inner 1s electron's wavefunctions have to include screening effects and to keep a hydrogen-like wavefunction shape.

For inner electrons it is reasonable to assume that, in the absence of an external electromagnetic field, their charge distribution could be fitted by a coulombian-like distribution. In this case, a coulombian field generated by the effective charge  $Z_{\text{ef}}(n, l)$  is acting on the  $nl$  subshell electron. This effective charge is that "seen" by an electron located at a distance from the nucleus given by the distance  $r_{\text{max}}^{\text{HF}}$  corresponding to the location of the single maximum of Hartree-Fock distribution in the case of 1s or 2p subshells and to the most important maximum in the case of 2s subshell. So, we have the static value of the effective charge "seen" by an  $nl$  electron

$$Z_{\text{ef}}^{\text{st}}(n, l) = Z - \sigma_{nl}^{\text{st}}, \quad (3.1)$$

where  $\sigma_{nl}^{\text{st}}$  is the static screening constant

$$\sigma_{nl}^{\text{st}} = \int_0^{r_{\text{max}}^{\text{HF}}} dr \rho_{nl}^{\text{HF}}(r). \quad (3.2)$$

The relation (3.1) highlights the coulombian field which is acting on the  $nl$  inner subshell electron, if no electromagnetic field is present, *i.e.* in the static regime. Hartree-Fock calculations show that in the K shell case, in the static regime, the screening constant  $\sigma_{1s}^{\text{st}}$  is almost independent of the atomic number  $Z$  and its value is approximatively 0.4.

The replacement of the Hartree-Fock charge distribution with a hydrogen-like charge distribution characterised by an effective charge  $Z_{\text{ef}}(n, l)$  given by the equations (3.1) and (3.2) is adequate to describe the interaction processes, because for a wide range of small momentum transfers of the incident photon the interaction occurs at large distances from nucleus, centered on the maximum of the charge distribution where the electron is most probably confined. This suggests a weak dependence of interacting distances on momentum transfer in the small energy incident photon case. Consequently, the effective charge that gives the coulombian field in the point of interaction can be assumed as slow dependant of the momentum transfer in the low energies case. On the contrary, in the case of energies well above the photoeffect threshold energy  $\omega_{1s}$ , the region where interaction takes place is increasingly close to the nucleus, the screening effects become weaker and the central field which is acting on the electron is described by an effective charge closer to  $Z$ .

Once the effective charge giving the hydrogen-like charge distribution is obtained from (3.1, 3.2), the energy of the bound 1s electron is given by

$E_{1s} = \gamma_{\text{ef}} m$ , where  $\gamma_{\text{ef}} = (1 - \alpha^2 Z_{\text{ef}}^2)^{\frac{1}{2}}$ . Also, the threshold energy  $\omega_{1s} = (1 - \gamma_{\text{ef}})m$  from which the parameters  $X(\Omega_1)$  and  $\tau(\Omega_1)$  become imaginary and the Rayleigh amplitude has an imaginary part, is determined. The value  $\omega = \omega_{1s}$  of the incident photon energy represents the threshold energy of the photoeffect on 1s shell.

Our screening model for Rayleigh scattering and the photoeffect in the case of inner electrons is based on the following considerations:

1. For low energies of the incident photon, *i.e.* for energies  $\omega \leq \omega_{1s}$ , the effective charge  $Z_{\text{ef}}(n, l, |\vec{\Delta}|)$  has the static value  $Z_{\text{ef}}^{\text{st}}(n, l)$ , which is obtained using the Hartree-Fock distribution for all values of the scattering angle  $\theta$

$$Z_{\text{ef}}(n, l, |\vec{\Delta}|) = Z_{\text{ef}}^{\text{st}}(n, l) = Z - \int_0^{r_{\text{max}}^{\text{HF}}} dr \rho_{nl}^{\text{HF}}. \quad (3.3)$$

Particularly, it follows that the static value of the effective charge represents the effective charge at the threshold energy,

$$Z_{\text{ef}}(n, l, \omega) = Z_{\text{ef}}^{\text{st}}(n, l), \quad \omega \leq \omega_{1s}. \quad (3.4)$$

2. If the photon energy  $\omega$  is above the threshold energy, but  $|\vec{\Delta}| \leq \omega_{1s}$  it is considered that  $Z_{\text{ef}}(n, l, |\vec{\Delta}|) = Z_{\text{ef}}^{\text{st}}(n, l)$ , therefore the effective charge is also given by its Hartree-Fock static value.

3. In the case of nodeless subshells ( $l = l_{\text{max}} = n - 1$ ), for incident photon energies greater than threshold energy  $\omega_{1s}$  and momentum transfer  $|\vec{\Delta}| > \omega_{1s}$ , the effective charge  $Z_{\text{ef}}(|\vec{\Delta}|)$ , which corresponds to the coulombian field acting on the electron, is obtained by knowing the distance  $r_{\text{max}}^{\text{ff}}$  from nucleus of the maximum of the atomic form factor integrand given by the Hartree-Fock charge distribution

$$Z_{\text{ef}}(n, n - 1, |\vec{\Delta}|) = Z - \int_0^{r_{\text{max}}^{\text{ff}}(|\vec{\Delta}|)} \rho_{n, n-1}^{\text{HF}} dr, \quad \omega_{1s} < |\vec{\Delta}| \leq 2\omega. \quad (3.5)$$

We point out that the distances from the nucleus which give contributions to the atomic form factor are centered on a maximum located at a known  $r_{\text{max}}^{\text{ff}}$ . It is reasonable to assume that the electron which interacts with the photon appears to be under the influence of a coulombian field due to the effective charge  $Z_{\text{ef}}(n, l, |\vec{\Delta}|)$  given by the eq. (3.5).

4. The *same* effective charge which is given by the atomic form factor and which occurs in the real part of the amplitude is involved in the imaginary part of the scattering amplitude, for a given value of momentum transfer.

In the following we show how the screening model works in the case of elastic scattering by a K-shell electron. The nonrelativistic expression of the form

factor  $\mathcal{O}_{ns}$  which gives the main contribution to the real part of the Rayleigh scattering amplitude is

$$\mathcal{O}_{ns} = \int_{\mathbb{R}^3} d^3r e^{i\vec{\Delta}\vec{r}} u_{ns}^2(r) = \frac{1}{|\vec{\Delta}|} \int_0^\infty dr r R_{n0}^2(r) \sin |\vec{\Delta}|r. \quad (3.7)$$

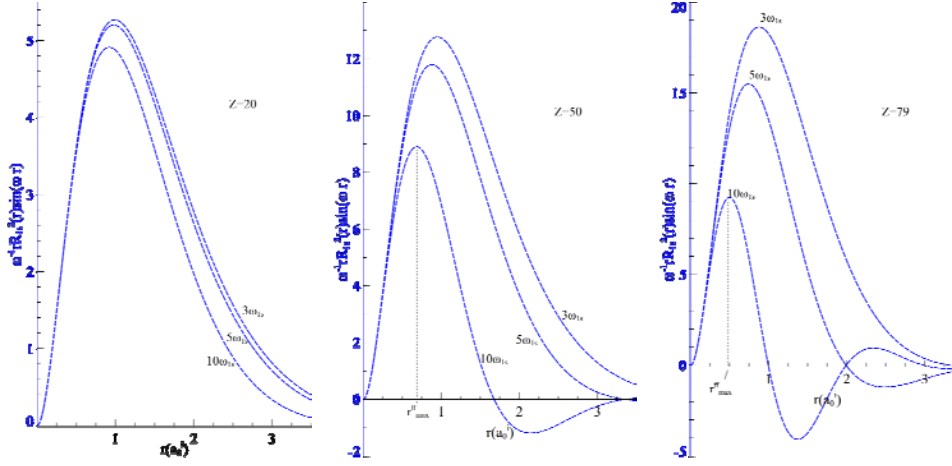


Fig. 2 – The integrand of the form factor (3.7) for Rayleigh scattering on 1s electron of a neutral atom of Calcium (Ca,  $Z=20$ ), Tin (Sn,  $Z=50$ ) and, respectively, Gold (Au,  $Z=79$ ), for different energies of the incident photon and the same scattering angle  $\theta = 60^\circ$ .

In Fig. 2 are showed the cases of Rayleigh scattering on the electron from K shell, for neutral atom of Calcium, Tin and Gold, for several energies of the incident photon, above the threshold energy of photoeffect ( $\omega = 3\omega_{1s}$ ,  $\omega = 5\omega_{1s}$  and  $\omega = 10\omega_{1s}$ ), and at the fixed scattering angle  $\theta = \frac{\pi}{3}$ , *i.e.* for the same momentum transfer  $|\vec{\Delta}| = \omega$  as in the case of photoeffect. Fig. 2 gives the exact location of the maximum of the integrand of the atomic form factor  $\mathcal{O}_{1s}$  for a given photon momentum transfer  $|\vec{\Delta}| > \omega_{1s}$ . The distances which give the main contribution to the form factor and to the real part of the Rayleigh amplitude belong to a narrow range centered on the maximum. An effective charge

$$Z_{\text{ef}}^{ns}(|\vec{\Delta}|) = Z - \int_0^{r_{\text{max}}^{\text{ff}}(|\vec{\Delta}|)} dr \rho_{\text{HF}}^{ns}(r) \quad (3.8)$$

corresponds to the abscissa  $r_{\text{max}}^{\text{ff}}(\vec{\Delta})$  of the maximum. This charge is the charge “seen” by the interacting electron, so we consider for the 1s electron a hydrogen-like charge distribution described by the screened charge  $Z_{\text{ef}}^{1s}(|\vec{\Delta}|)$ .

Table 1

Rayleigh scattering for Calcium ( $Z=20$ ,  $\omega = 8.048$  keV – left and  $\omega = 27.47$  keV – right).  
(the cross sections are given in units of  $10^{-26}$  cm $^2$ )

$\theta$	$A^{\parallel}$	$A^{\perp}$	$\frac{d\sigma}{d\Omega}$	$R_{\parallel}^{\text{im}}$	$R_{\parallel}^{\text{re}}$	$R_{\perp}^{\text{im}}$	$R_{\perp}^{\text{re}}$	$A^{\parallel}$	$A^{\perp}$	$\frac{d\sigma}{d\Omega}$	$R_{\parallel}^{\text{im}}$	$R_{\parallel}^{\text{re}}$	$R_{\perp}^{\text{im}}$	$R_{\perp}^{\text{re}}$
0	2.42-1.18i	2.42-1.18i	57.6	91.2	11.9	91.2	11.9	2.13-0.12i	2.13-0.12i	36.1	91.3	10.6	91.3	10.6
10	2.39-1.15i	2.42-1.18i	56.7	90.9	12.5	91.0	12.5	2.09-0.11i	2.12-0.11i	35.4	90.1	14.3	91.1	14.3
20	2.27-1.10i	2.42-1.17i	54.1	90.7	13.9	91.0	13.9	1.98-0.10i	2.11-0.11i	33.3	89.6	20.6	91.1	20.6
30	2.09-1.01i	2.42-1.17i	50.1	90.6	15.3	90.9	15.3	1.80-0.09i	2.09-0.11i	30.3	89.4	26.7	91.1	26.8
40	1.85-0.89i	2.42-1.17i	45.3	90.6	16.9	90.9	16.9	1.57-0.08i	2.06-0.11i	26.7	89.4	31.1	91.2	31.2
50	1.55-0.74i	2.41-1.17i	40.3	90.6	18.7	90.9	18.7	1.29-0.07i	2.03-0.11i	23.0	89.8	35.4	91.3	35.6
60	1.20-0.57i	2.41-1.17i	35.5	90.7	20.6	90.9	20.5	0.98-0.05i	1.99-0.11i	19.6	90.4	40.7	91.4	40.9
70	0.82-0.38i	2.41-1.16i	31.6	90.8	22.5	91.0	22.4	0.65-0.03i	1.95-0.11i	16.8	91.5	47.1	91.6	47.4
80	0.42-0.19i	2.40-1.16i	29.1	91.0	24.3	91.0	24.2	0.32-0.01i	1.91-0.11i	14.9	94.5	54.2	91.7	54.6
90	0.00+0.01i	2.40-1.16i	28.2	88.7	13.5	91.0	25.8	-0.01+0.01i	1.86-0.11i	13.8	86.1	63.7	91.8	61.9
100	-0.42+0.22i	2.39-1.16i	28.9	90.9	27.1	91.0	27.2	-0.33+0.03i	1.82-0.11i	13.7	90.6	68.7	91.9	68.9
110	-0.82+0.41i	2.39-1.15i	31.3	91.1	28.3	91.0	28.4	-0.62+0.04i	1.78-0.10i	14.2	92.0	74.9	92.0	75.0
120	-1.19+0.59i	2.38-1.15i	34.9	91.2	29.3	91.0	29.3	-0.89+0.06i	1.75-0.10i	15.3	92.8	80.1	92.1	80.2
130	-1.53+0.75i	2.38-1.15i	39.3	91.3	30.1	91.0	30.1	-1.11+0.07i	1.72-0.10i	16.7	93.4	84.3	92.2	84.3
140	-1.82+0.89i	2.38-1.15i	44.0	91.4	30.7	91.0	30.7	-1.30+0.08i	1.69-0.10i	18.2	93.8	87.5	92.3	87.4
150	-2.06+1.00i	2.38-1.15i	48.4	91.4	31.2	91.0	31.2	-1.45+0.09i	1.67-0.10i	19.6	93.9	89.8	92.3	89.7
160	-2.23+1.08i	2.37-1.15i	52.0	91.3	31.5	91.0	31.5	-1.56+0.10i	1.66-0.10i	20.7	93.7	91.3	92.4	91.2
170	-2.34+1.13i	2.37-1.15i	54.3	91.2	31.7	91.0	31.7	-1.62+0.10i	1.65-0.10i	21.3	93.2	92.1	92.4	92.0
180	-2.37+1.15i	2.37-1.15i	55.1	91.0	31.7	91.0	31.7	-1.64+0.10i	1.64-0.10i	21.6	92.4	92.3	92.4	92.3

Table 2

Rayleigh scattering for Tin ( $Z=50$ ,  $\omega = 36.03$  keV – left and  $\omega = 77.11$  keV – right).  
(the cross sections are given in units of  $10^{-26}$  cm $^2$ )

$\theta$	$A^{\parallel}$	$A^{\perp}$	$\frac{d\sigma}{d\Omega}$	$R_{\parallel}^{\text{im}}$	$R_{\parallel}^{\text{re}}$	$R_{\perp}^{\text{im}}$	$R_{\perp}^{\text{re}}$	$A^{\parallel}$	$A^{\perp}$	$\frac{d\sigma}{d\Omega}$	$R_{\parallel}^{\text{im}}$	$R_{\parallel}^{\text{re}}$	$R_{\perp}^{\text{im}}$	$R_{\perp}^{\text{re}}$
0	1.96-2.25i	1.96-2.25i	70.4	88.9	4.0	88.9	4.0	2.24-0.59i	2.24-0.59i	42.5	88.1	4.5	88.1	4.5
10	1.93-2.20i	1.96-2.24i	69.2	88.5	5.3	88.9	5.3	2.19-0.56i	2.23-0.58i	41.4	85.7	8.9	87.5	8.9
20	1.85-2.07i	1.95-2.23i	65.5	87.9	7.7	88.4	7.6	2.07-0.51i	2.22-0.58i	38.9	84.5	14.1	87.4	14.2
30	1.72-1.89i	1.95-2.22i	60.5	87.7	10.2	88.3	10.0	1.88-0.45i	2.19-0.57i	35.2	84.1	21.4	87.5	21.5
40	1.53-1.65i	1.95-2.21i	54.5	87.8	12.5	88.3	12.2	1.63-0.38i	2.16-0.56i	30.8	84.5	30.8	87.7	30.9
50	1.29-1.36i	1.95-2.20i	48.2	88.2	15.1	88.4	14.6	1.33-0.29i	2.11-0.55i	26.4	85.6	38.1	88.0	38.0
60	1.01-1.03i	1.94-2.19i	42.3	88.9	18.7	88.5	17.7	1.01-0.20i	2.07-0.54i	22.3	87.8	43.5	88.2	42.9
70	0.71-0.68i	1.94-2.18i	37.6	90.0	23.3	88.6	21.4	0.66-0.11i	2.02-0.53i	19.1	92.7	49.2	88.5	47.8
80	0.38-0.31i	1.94-2.17i	34.5	93.1	30.2	88.7	25.3	0.31-0.02i	1.97-0.51i	16.8	167.5	58.1	88.8	53.4
90	0.05+0.07i	1.93-2.15i	33.3	72.1	-79.3	88.8	29.1	-0.03+0.07i	1.92-0.50i	15.6	77.7	29.1	89.1	59.5
100	-0.29+0.44i	1.93-2.14i	34.1	86.2	26.7	89.0	32.3	-0.35+0.15i	1.87-0.49i	15.4	84.5	60.2	89.3	65.7
110	-0.62+0.79i	1.93-2.13i	36.8	88.0	32.1	89.1	35.1	-0.65+0.22i	1.82-0.48i	16.0	87.6	68.3	89.5	71.6
120	-0.92+1.12i	1.92-2.12i	40.9	88.9	35.3	89.2	37.3	-0.91+0.29i	1.78-0.47i	17.1	89.7	74.7	89.6	76.8
130	-1.20+1.41i	1.92-2.11i	45.9	89.5	37.6	89.2	39.0	-1.14+0.34i	1.75-0.46i	18.6	91.2	79.8	89.8	81.1
140	-1.44+1.65i	1.92-2.10i	51.3	89.8	39.4	89.3	40.4	-1.33+0.38i	1.72-0.45i	20.1	92.2	83.8	89.8	84.6
150	-1.64+1.85i	1.91-2.10i	56.2	90.0	40.8	89.4	41.4	-1.48+0.41i	1.69-0.44i	21.5	92.6	86.8	89.9	87.1
160	-1.78+1.99i	1.91-2.09i	60.3	90.0	41.7	89.4	42.1	-1.58+0.43i	1.68-0.44i	22.6	92.5	88.8	90.0	88.8
170	-1.88+2.07i	1.91-2.09i	62.8	89.8	42.4	89.4	42.6	-1.64+0.44i	1.67-0.44i	23.3	91.6	89.9	90.0	89.8
180	-1.91+2.09i	1.91-2.09i	63.7	89.4	42.7	89.4	42.7	-1.66+0.44i	1.66-0.44i	23.4	90.0	90.2	90.0	90.2

In the case of a momentum transfer  $|\vec{\Delta}| = \omega$ , the effective charge  $Z_{\text{ef}}^{1s}(\omega)$  calculated with the integral (3.8) is presented in the Table 4 for different neutral atoms.

The correctness of our screening model may be checked by comparing numerical predictions which are based on this model with the most accurate numerical data that are given in literature in the case of the elastic scattering of photons by a free atom [9]. In Tables 1-3 we present the contribution  $A^{\parallel}$  and  $A^{\perp}$  of the K-shell electrons to the amplitudes  $A_{\text{atom}}^{\parallel}$  and  $A_{\text{atom}}^{\perp}$  of the Rayleigh scattering given by the coherent sum of the amplitudes of all electrons of the atom [9]. The contribution to the angular distribution of unpolarized photons scattered by the K-shell electrons is given by

$$\frac{d\sigma}{d\Omega} = \frac{1}{2} (|A^{\parallel}|^2 + |A^{\perp}|^2) r_0^2. \quad (3.9)$$

By definition, the ratios  $R_{\parallel}^{\text{re}}$ ,  $R_{\parallel}^{\text{im}}$ ,  $R_{\perp}^{\text{re}}$  and  $R_{\perp}^{\text{im}}$  showed in the Tables 1–3 are

$$R_{\parallel}^{\text{re}} = \frac{\text{Re}A^{\parallel}}{\text{Re}A_{\text{atom}}^{\parallel}}; \quad R_{\parallel}^{\text{im}} = \frac{\text{Im}A^{\parallel}}{\text{Im}A_{\text{atom}}^{\parallel}}; \quad R_{\perp}^{\text{re}} = \frac{\text{Re}A^{\perp}}{\text{Re}A_{\text{atom}}^{\perp}}; \quad R_{\perp}^{\text{im}} = \frac{\text{Im}A^{\perp}}{\text{Im}A_{\text{atom}}^{\perp}}. \quad (3.10)$$

Table 3

Rayleigh scattering for Gold ( $Z=79$ ,  $\omega = 98.44$  keV – left and  $\omega = 145.4$  keV – right ).  
(the cross sections are given in units of  $10^{-26}$  cm<sup>2</sup>)

$\theta$	$A^{\parallel}$	$A^{\perp}$	$\frac{d\sigma}{d\Omega}$	$R_{\parallel}^{\text{im}}$	$R_{\parallel}^{\text{re}}$	$R_{\perp}^{\text{im}}$	$R_{\perp}^{\text{re}}$	$A^{\parallel}$	$A^{\perp}$	$\frac{d\sigma}{d\Omega}$	$R_{\parallel}^{\text{im}}$	$R_{\parallel}^{\text{re}}$	$R_{\perp}^{\text{im}}$	$R_{\perp}^{\text{re}}$
0	1.57-2.01i	1.57-2.01i	51.7	86.5	2.0	86.5	2.0	1.98-1.01i	1.98-1.01i	39.1	82.4	2.5	82.4	2.5
10	1.57-1.95i	1.57-2.01i	50.7	85.5	4.2	86.5	4.2	1.95-0.95i	1.97-1.00i	38.1	79.5	7.2	82.0	7.1
20	1.53-1.80i	1.56-1.98i	47.3	84.0	8.3	85.6	7.9	1.86-0.85i	1.95-0.98i	35.5	77.3	14.0	81.3	13.8
30	1.43-1.60i	1.56-1.95i	43.2	83.6	12.4	85.4	11.6	1.70-0.73i	1.93-0.96i	32.0	76.8	21.3	81.5	20.7
40	1.30-1.37i	1.56-1.93i	38.6	84.0	16.9	85.6	15.3	1.49-0.59i	1.90-0.94i	27.9	77.3	32.5	82.0	31.0
50	1.12-1.10i	1.56-1.91i	33.8	84.8	23.9	85.9	20.8	1.23-0.44i	1.86-0.91i	23.8	78.8	42.5	82.7	39.4
60	0.91-0.80i	1.55-1.89i	29.5	86.3	33.6	86.3	27.5	0.94-0.28i	1.81-0.89i	20.0	81.8	50.9	83.3	45.2
70	0.67-0.48i	1.55-1.86i	25.9	88.9	45.8	86.7	33.6	0.64-0.13i	1.76-0.86i	17.0	90.0	62.2	84.0	50.9
80	0.41-0.15i	1.54-1.83i	23.6	99.2	69.5	87.1	38.4	0.33+0.02i	1.72-0.83i	14.9	47.7	91.6	84.5	57.5
90	0.14+0.16i	1.54-1.81i	22.5	77.8	-141.2	87.4	42.3	0.03+0.16i	1.67-0.80i	13.7	75.7	-23.4	85.0	64.9
100	-0.14+0.47i	1.54-1.78i	22.9	84.8	20.4	87.7	45.9	-0.25+0.29i	1.62-0.77i	13.4	80.7	48.5	85.3	72.3
110	-0.40+0.75i	1.53-1.75i	24.4	87.1	35.7	87.9	49.4	-0.51+0.39i	1.58-0.75i	13.8	83.9	64.7	85.6	79.0
120	-0.65+1.00i	1.53-1.73i	26.8	88.5	43.9	88.0	53.0	-0.75+0.49i	1.54-0.73i	14.7	86.3	75.0	85.8	84.8
130	-0.88+1.22i	1.52-1.71i	29.8	89.4	49.9	88.0	56.3	-0.95+0.56i	1.51-0.71i	15.8	88.1	82.5	85.9	89.4
140	-1.09+1.40i	1.52-1.69i	33.0	90.0	54.8	88.1	59.4	-1.12+0.61i	1.48-0.69i	17.0	89.3	88.3	85.9	92.8
150	-1.25+1.53i	1.52-1.68i	35.9	90.1	58.8	88.1	62.0	-1.25+0.65i	1.46-0.68i	18.1	89.8	92.4	85.9	95.2
160	-1.38+1.62i	1.51-1.67i	38.2	89.9	62.0	88.1	63.9	-1.35+0.67i	1.44-0.67i	19.0	89.5	95.5	85.9	96.7
170	-1.47+1.66i	1.51-1.66i	39.6	89.2	64.2	88.1	65.2	-1.40+0.67i	1.43-0.66i	19.5	88.2	97.0	85.9	97.8
180	-1.51+1.66i	1.51-1.66i	40.0	88.0	65.5	88.0	65.5	-1.43+0.66i	1.43-0.66i	19.6	85.9	97.9	85.9	97.9

### 3.2. THE SCREENING MODEL FOR PHOTOEFFECT ON 1S ELECTRONS

As we already mentioned, the effective charge  $Z_{\text{ef}}(\omega)$  in the case of photoeffect equals the effective charge which corresponds to Rayleigh scattering, at the same incident photon energy  $\omega$  and at the scattering angle  $\theta = \frac{\pi}{3}$ . As we know, based on the optical theorem, in the hydrogen-like case, the total cross section of the photoelectric effect is associated with the imaginary part of Rayleigh scattering amplitude which corresponds to forward scattering ( $\theta = 0$ ) and with the particularity  $\vec{s}_1 = \vec{s}_2$ . It is normal to assume that the above statement remain true in the multielectron atom case, in which case the atomic charge should be replaced by the dynamic value of the effective charge, which is determined by the screening model of the elastic scattering effect.

Table 4 shows the good agreement between the values for our photoeffect cross section and Scofield results [7] for photon energies even larger than  $\alpha Zm$ .

Table 4

K-shell photoeffect cross section for neutral atom of Calcium (Ca), Tin (Sn) and Gold (Au). The column “ $\delta$ ” gives the relative discrepancy between our and Scofield photoeffect cross sections

$\omega$ [keV]	$Z_{\text{ef}}$	$\sigma^{\text{Scof}}$ [barn]	$\sigma^{\text{ph}}$ [barn]	$\delta$ [%]	$\omega$ [keV]	$Z_{\text{ef}}$	$\sigma^{\text{Scof}}$ [barn]	$\sigma^{\text{ph}}$ [barn]	$\delta$ [%]	$\omega$ [keV]	$Z_{\text{ef}}$	$\sigma^{\text{Scof}}$ [barn]	$\sigma^{\text{ph}}$ [barn]	$\delta$ [%]
5	19.61	35714	-	-	30	49.59	6700.1	-	-	92.43	78.59	-	1640.6	-
5.26	19.61	-	32567	-	34.59	49.59	-	4789.7	-	100	78.59	1272.5	1317.9	3.6
6	19.61	22176	22812	2.9	40	49.59	3160.3	3221.5	1.9	125	78.59	-	710.7	-
8	19.61	10285	10364	0.8	50	49.59	1730.8	1744.3	0.8	150	78.60	441.6	430.6	-2.5
10	19.62	5559.6	5547.6	-0.2	60	49.60	1051	1053	0.2	175	78.61	-	282.74	-
15	19.62	1756.9	1737.1	-1.1	80	49.61	470.6	472.9	0.5	200	78.63	205.69	196.86	-4.3
20	19.62	758.27	749.53	-1.2	100	49.62	249.72	253.60	1.6	250	78.65	-	108.12	-
30	19.63	225.74	225.23	-0.2	125	49.63	-	136.00	-	300	78.67	70.925	66.647	-6.0
40	19.64	93.964	95.092	1.2	150	49.65	77.92	81.83	5.0	350	78.70	-	44.462	-
50	19.66	47.234	48.569	2.8	200	49.69	34.092	36.859	8.1	400	78.73	34.215	31.413	-8.2
60	19.68	26.812	28.032	4.6	300	49.77	10.865	12.131	11.7	450	78.75	-	23.178	-
80	19.71	10.906	11.785	8.1	400	49.83	4.9876	5.5771	11.8	500	78.77	19.905	17.693	-11.1
Z=20; $\omega_{1s}=5.25$ keV					Z=50; $\omega_{1s}=34.59$ keV					Z=79; $\omega_{1s}=92.40$ keV				

## 5. CONCLUSIONS

Numerical results presented in Tables 1-3 show that for large momentum transfer  $|\vec{\Delta}|$  the K shell electrons give at least 80% from the contribution of the whole atom to the elastic scattering amplitude, in a good agreement with other authors [1, 2]. The next important contribution at a large momentum transfers, about 15–18% to the coherent sum of the electron amplitudes, comes from the L shell electrons [1].

The good predictions for the photoeffect cross section show that the imaginary part of the Rayleigh amplitudes is obtained with high accuracy, *i.e.* the dependence on the photon energy due to multipoles, retardation and relativistic kinematics is correctly taken into account.

*Acknowledgments.* This work was supported by the Romanian National Research Authority (ANCS) under Grant PNII 71-002/2007.

## REFERENCES

1. L. Kissel, R.H. Pratt and S. C. Roy, Phys. Rev. A, **22**, 1970 (1980);  
P.P. Kane, L. Kissel, R.H. Pratt and S. C. Roy, Phys. Rep., **140**, 75 (1986).
2. J.P.J. Carney, R. H. Pratt, L. Kissel, S. C. Roy and S. K. Sen Gupta, Phys. Rev. A, **61**, 052714 (2000).
3. T. Surić, P. M. Bergstrom, Jr., K. Pisk and R.H. Pratt, Phys. Rev. Lett., **67**, 189 (1991);  
P. M. Bergstrom, Jr., T. Surić, K. Pisk and R. H. Pratt, Phys. Rev. A, **48**, 1134 (1993).
4. A. Costescu, S. Spanulescu and C. Stoica, J. Phys. B: At. Mol. Opt. Phys., **40**, 2995 (2007).
5. A. Costescu, S. Spanulescu, Phys. Rev. A, **73**, 022702 (2006).
6. L.A. LaJohn, Phys. Rev. A, **81**, 043404 (2010).
7. J.H. Scofield, *Lawrence Radiation Laboratory*, Report No. CRL 51326, Livermore CA, unpublished, 1973.
8. S. Hultberg, B. Nagel and P. Olsson, Ark. Fys., **38**, 1 (1968).
9. L. Kissel, Radiation Physics and Chemistry, **59**, 185 (2000).